JOURNAL OF APPLIED ELECTROCHEMISTRY **29** (1999) 277–283.

Electrochemical degradation of phenol in aqueous solution on bismuth doped lead dioxide: a comparison of the activities of various electrode formulations

N. BELHADJ TAHAR, A. SAVALL*

Laboratoire de Génie Chimique, CNRS UMR 5503, Université Paul Sabatier, 118, Route de Narbonne, 31062 Toulouse cedex, France
*(*author for correspondence, e-mail: savall@ramses.ups-tlse.fr)*

Received 27 January 1998; accepted in revised form 28 April 1998

This paper describes the development of electrochemical processes for the oxidative degradation of toxic organic chemicals in waste waters. Doped bismuth lead dioxide anodes have been tested by the kinetic study of phenol anodic oxidation in aqueous solution. The main products during oxidative degradation of phenol are 1,4-benzoquinone, maleic acid and carbon dioxide. Several deposits of Bi_2O_5–PbO_2 on Ti/(IrO_2–Ta_2O_5) substrates have been prepared by anodic oxidation of Pb^{2+} and Bi^{3+} in aqueous solutions containing perchloric acid to increase the solubility of bismuth. To study the effect of perchlorate ions, the efficiency of the PbO_2 deposit prepared from lead nitrate in an aqueous solution (pure PbO_2) was compared with that of a deposit prepared from perchloric acid solution (perchlorate doped PbO_2). Although the phenol is oxidized at the same rate on the two deposits, the charge corresponding to the total elimination of 1,4-benzoquinone is three times higher for perchlorate doped PbO_2 than for pure PbO_2. Phenol degradation is more efficiently carried out on a PbO_2 anode doped with perchlorate and with bismuth than on the same electrode doped only with perchlorate. Among the electrodes tested in this work, the pure PbO_2 anode is the most efficient for phenol degradation. It is assumed that certain active sites on the anode occupied by perchlorate ions do not participate in the transfer of oxygen atoms and that for the PbO_2 electrode doped with bismuth, oxygen evolution is favoured to the detriment of oxygen atom transfer.

Keywords: *waste water treatments*, *oxidative degradation*, *phenol oxidation*, *PbO_2 anode*, *bismuth doping*

1. Introduction

Industrial effluents containing toxic and/or biorefractory products are presently a serious environmental problem due to the increasing severity of the legislation on acceptable limits and to the lack of general treatment methods. Among aqueous industrial effluents, those containing organic pollutants cause problems due to the high activation energy barrier for chemical oxidation reactions and to the complexity of the degradation mechanisms. The electrochemical method can be used for partial or total degradation of toxic organic substances. Many organic compounds in aqueous solution can be oxidized on an anode by direct electron or oxygen atom transfer; the oxidation can go right to the carbon dioxide and water via successive reactions each one has several steps: mass transport, adsorption, direct or indirect reaction at the surface of the electrode [1–5].

The electrochemical reactivity of each organic compound depends on the anode material used. In fact, while spontaneous, the oxidation reactions by oxygen transfer are characterized by low rate constants when carried out on traditional electrode materials such as Au, Pt, C... [1, 2, 6–12]. It is now thought that the step preceding the transfer of an oxygen atom in the oxidation mechanism of organic substances in aqueous solution is the discharge of the water molecule leading to an adsorbed hydroxyl radical [1, 13–17].

$$MO_x [\ ] + H_2O \rightarrow MO_x [OH^{\cdot}] + H^+ + e^- \quad (1)$$

The relative slowness of the oxygen atom transfer is due to the competing reaction forming molecular oxygen:

$$2\ MO_x [OH^{\cdot}] \rightarrow 2\ MO_x [\ ] + O_2 + 2\ H^+ + 2\ e^- \quad (2)$$

The use of an anode material with a high oxygen evolution overpotential favours the oxygen transfer. Lead dioxide fulfills this criteria, however, with the aim of improving the transfer rate of the oxygen atom, it was suggested that doping lead dioxide with metallic cations whose corresponding oxides have a low oxygen evolution overpotential. The work of Johnson *et al.* [15, 18, 19] has shown, on an analytical scale, that doping PbO_2 with bismuth noticeably improves the oxidation kinetics of several organic compounds. X-ray studies have shown that the electrochemical codeposition of the oxide mixture Bi_2O_5–

PbO_2 corresponds to a simple substitution of lead by bismuth in the crystalline network without changing its structure [19]. The catalytic effect obtained by doping PbO_2 with bismuth results from the formation of a low surface density of bismuth oxide (Bi_2O_5) sites characterized by a low oxygen evolution overpotential (ηO_2). By positively polarizing the Bi_2O_5–PbO_2 electrode, water decomposes preferentially on the sites of low ηO_2. For a low level of doping, the oxygen evolution rate on the Bi_2O_5 sites is negligeable; the adsorbed hydroxyl radicals, formed preferentially on the Bi_2O_5 sites, contribute to the oxygen transfer reactions taking place on the high ηO_2 (PbO_2) sites.

In this study, we have undertaken testing of the effect of doping lead dioxide with bismuth on the oxidative degradation rate of phenol in aqueous solution. This study has been carried out by liquid chromatography by assaying the intermediate products formed during the electrolysis of phenol and by measuring the total organic carbon value. Special attention has also been paid to the electrode stability during these electrolyses by checking the corrosion of the Bi_2O_5–PbO_2.

2. Experimental details

2.1. *Preparation of PbO_2 and Bi_2O_5–PbO_2 deposited on Ti(IrO_2–Ta_2O_5)*

The lead dioxide was deposited by electrochemical oxidation of a lead nitrate solution. The Bi_2O_5–PbO_2 layer was prepared electrochemically from a solution of lead nitrate and bismuth nitrate. Bismuth salts have a low solubility; the value for bismuth nitrate in water is around 10^{-3} mol dm^{-3} at 20 °C; however its solubility is higher in perchloric acid solution (Table 1); a 1 mol dm^{-3} $HClO_4$ solution has been used (Table 1). The solutions used for the preparation of PbO_2 and Bi_2O_5–PbO_2 contained in addition 0.12 mol dm^{-3} copper nitrate and a very small quantity (0.1 g dm^{-3}) of sodium dodecyl sulphate (SDS). The copper, less electropositive than the lead, is deposited preferentially on the cathode and inhibits the formation of lead dendrites. The presence of the SDS in solution improves the adhesion at the substrate/ PbO_2 interface and increases the specific surface deposit [20–23]. The PbO_2 and Bi_2O_5–PbO_2 deposits were prepared on rectangular plates of titanium (70 mm × 10 mm × 1 mm). Titanium has good chemical and electrochemical stability.

2.1.1. Surface treatment. The titanium plates were first roughened to increase the adhesion of the PbO_2 deposit. The surface of the titanium was subjected to mechanical abrasion by sand blasting with grains of 0.3 mm average diameter at a pressure of 5 bar (Brasfanta 037/320 Bremor, Switzerland). The titanium substrate was then cleaned using ultrasound for 10 min to remove any sand particles lodged in the metal. The average loss in mass per unit of surface area due to the sand blasting was 0.16 ± 0.05 mg cm^{-2}. Then, chemical etching was

Table 1. Experimental conditions for preparation of PbO_2 and Bi_2O_5–PbO_2 electrodeposited on a Ti/(IrO_2–Ta_2O_5) substrate

T = 65 °C, [$Cu(NO_3)_2$] = 0.12 mol dm^{-3} and [SDS] = 0.1 g dm^{-3}

Deposit	*Solvent*	[Pb^{2+}]/M	$R_c = \frac{[Bi^{3+}]}{[Pb^{2+}]}$	J/mA cm^{-2}	*Time*/min	*Observations*
1	H_2O	1	0	100	30	Porous and uniform coating.
2	$HClO_4$ 1 M	1	0	100	30	Irregular, porous but adherent coating.
3	$HClO_4$ 1 M	0.5	0.02	40	30	Porous, mat grey, adherent and non uniform coating.
4	H_2O	1	0	100	15	1st PbO_2 layer on Ti/IrO_2–Ta_2O_5
	$HClO_4$ 1 M	0.2	0.5	40	30	2nd Bi–PbO_2 layer on PbO_2 Porous, shine, grey and adherent coating. Small, regular and uniform granulometry.
5	H_2O	1	0	100	15	1st PbO_2 layer on Ti/IrO_2–Ta_2O_5
	$HClO_4$ 1 M	0.5	0.1	40	30	2nd Bi–PbO_2 layer on PbO_2
	H_2O	1	0	100	15	3rd PbO_2 layer on Bi–PbO_2 Very porous, mat grey, adherent, uniform and regular coating.
6	H_2O	1	0	100	15	1st PbO_2 layer on Ti/IrO_2–Ta_2O_5
	$HClO_4$ 1 M	0.2	0.5	40	30	2nd Bi–PbO_2 layer on PbO_2
	H_2O	1	0	100	15	3rd PbO_2 layer on Bi–PbO_2 Very porous, mat grey, adherent, uniform and regular coating.
7	H_2O	0.5	2×10^{-4}	100	30	Very porous, mat grey, adherent and uniform coating.
8	H_2O	0.5	2×10^{-3}	100	30	Very porous, mat grey, adherent, uniform and regular coating.

carried out using boiling concentrated hydrochloric acid (32% by mass) for 30 min. The titanium plates were then washed in distilled water. The loss in mass per unit of surface area due to this chemical treatment was 13.07 ± 1.85 mg cm^{-2}.

2.1.2. Deposition of a layer of conducting oxides using thermal treatment. The stripped titanium substrate was then covered with a mixture of insoluble and electrically conductive metal oxides (IrO_2–Ta_2O_5), to prevent passivation through the formation of a non-conducting film of TiO_2. This mixture of metallic oxides was obtained by the thermal decomposition technique. A solution was firstly prepared by dissolving successively 280 mg of tantalum pentachloride ($TaCl_5$) and 480 mg of hexachloroiridic acid (H_2IrCl_6, $6\,H_2O$) in a mixture of 5 cm^3 of absolute ethanol and 5 cm^3 of isopropanol. This solution was brushed onto the titanium base, then the solvent was evaporated at 60 °C. The electrode then underwent a thermal decomposition in an oven for 10 min at 530 °C in an air atmosphere and was then cooled. This operations sequence (painting, evaporation and thermal treatment) was repeated 10 times. The final stage consisted of heating in air to 530 °C for 2 h. The average mass of tantalum and iridium oxides deposited per unit of surface area was 0.95 ± 0.16 mg cm^{-2}. The mixture of precursors used allows to form a mixture of oxides (IrO_2–Ta_2O_5) in the molar proportions 70–30%, respectively [24].

2.1.3. Electrochemical deposition of PbO_2 and Bi_2O_5–PbO_2. PbO_2 and Bi_2O_5–PbO_2 were deposited galvanostatically onto the layer of tantalum and iridium oxides (IrO_2–Ta_2O_5). They were prepared in a single compartment cell (V = 200 cm^3) thermostated at 65 °C. The cathode used was a cylindrical mesh made of Pt–Ir alloy (ϕ = 5 cm and L = 5 cm). The two electrodes were concentric; the Ti/(IrO_2–Ta_2O_5) anode was axial. This arrangement gave the formation of a regular and uniform deposit. The different operating conditions used for the preparation of the PbO_2 and Bi_2O_5–PbO_2 deposits were grouped together in Table 1. The average mass of PbO_2 deposited per unit of surface area was 0.2 g cm^{-2}; the average faradaic yield was 93.3%.

2.2. *Electrolyses*

The electrolyses of the acidic aqueous phenol solutions were carried out in a two compartment, isothermal reactor. The electrolytes to be treated, volume 160 cm^3, contained phenol at an initial concentration of 21 mmol dm^{-3}. The pH of the solution was adjusted to 2 by adding sulphuric acid initially to give a conducting medium and then to minimize the electrochemical polymerization reactions of the phenol which cause anode passivation [5, 7–9, 25, 26]. The homogeneous nature of the medium during the electrolyses was maintained using magnetic stirring. The electrolyses were carried out at 70 °C. The anode was made up of four identical plates (70 mm × 10 mm × 1 mm) arranged symmetrically around the cathode; the side of each plate not facing the cathode was covered with a protective film (transparent polyethylene tape, Scotch TM 480. 3M). The working surface area of each plate was 5 cm^2. The cathode was a graphite rod (ϕ = 1 cm; L = 6 cm) placed in a porous ceramic cylinder (Norton, Refractaire RA 84) containing 1 mol dm^{-3} sulphuric acid. The acid solutions of phenol were electrolysed galvanostatically using an anodic current density of 100 mA cm^{-2}. During the electrolyses, the pH of the anolyte has decreased from 2 to around 0.5.

2.3. *Analyses*

The quantitative and qualitative identification of the oxidation products of the phenol solutions was made by high pressure liquid chromatography using a Hewlett Packard 1090 apparatus. The products were separated on a PRP X 300, Hamilton column specifically for organic acids, and then analysed quantitatively using a diode array detector measuring the optical density at 220 nm at the column output (injection volume 20 μl). The mobile phase was a mixture of methanol and 5×10^{-2} mol dm^{-3} sulphuric acid with the percentage by volume of methanol varying linearly with time as follows: from 2 to 25% for the first ten minutes then from 25 to 40% up to 20 min and finally from 40 to 60% up to 40 min. The mobile phase flow rate was fixed at 1.3 ml min^{-1}.

The total organic carbon was measured using an O. I analytical model 700 TOC analyser. Samples of 0.5 ml were taken over the course of the electrolyses and were then diluted to bring their concentration within the operating range of the apparatus.

The amounts of lead and bismuth in solution were analysed using a JobinYvon JY24 ICP analyser. The wavelengths used for the lead and bismuth analyses were 220.353 and 223.061 nm, respectively. Detection limits for lead and bismuth were 42 and 34 μg dm^{-3} respectively.

3. Results and discussion

The properties of PbO_2 deposits prepared from lead nitrate in aqueous solution (deposit **1**) and in perchloric acid solution (deposit **2**) were compared relative to the phenol degradation. The main products formed during the electrochemical oxidation of an aqueous solution of phenol were 1,4-benzoquinone, maleic acid and carbon dioxide; the amount of phenol completely oxidized to carbon dioxide and water can be calculated from the total organic carbon measurement [5]. The other products found, present in low concentrations (less than 0.5 mmol dm^{-3}), were hydroquinone, catechol and fumaric acid.

From Fig. 1 it can be seen that phenol is oxidised at the same rate during electrolyses carried out using PbO_2 deposits **1** and **2**, and the same charge, about 20 Ah dm^{-3}, is needed for its complete consumption.

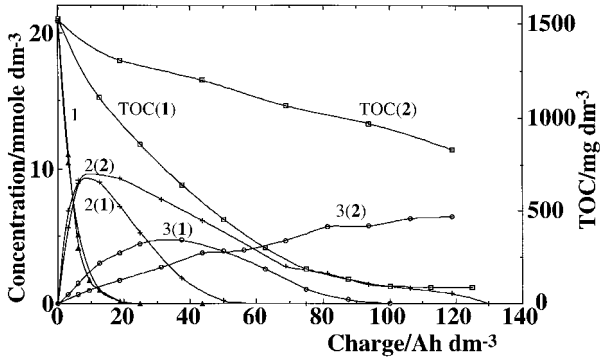

Fig. 1. Effect of the composition of the solution used for the preparation of PbO_2 for the degradation of phenol ($V = 160\,cm^3$) on PbO_2 anodes **1** and **2** ($S = 20\,cm^2$). Initial phenol concentration: $21\,mmol\,dm^{-3}$; anodic current density, $j = 100\,mA\,cm^{-2}$; temperature, $T = 70\,°C$; pH 2. Key: (1) phenol; (2(**1**) and 2(**2**)) 1,4-benzoquinone; (3(**1**) and 3(**2**)) maleic acid; (TOC(**1**) and TOC(**2**)) total organic carbon.

At the experiment outset (charge $< 10\,Ah\,dm^{-3}$), the two concentration curves for 1,4-benzoquinone are almost superimposed (Fig. 1); the 1,4-benzoquinone is therefore oxidised at the same rate on both deposits. However, the charge needed for the complete consumption of 1,4-benzoquinone was three times higher for deposit **2** (prepared from a perchloric acid electrolyte) than for deposit **1**. The phenol oxidation mechanism is discussed elsewhere [4, 5]; it is assumed from the faradaic yield and the TOC variation that, at the beginning of the electrolysis, adsorbed phenol molecules can undergo several oxidation steps going successively to hydroquinone, 1,4-benzoquinone, maleic acid and even carbon dioxide, probably without desorption of any intermediate products. The oxidation step to 8 electrons leading to the formation of maleic acid, is very probably attained by certain phenol molecules adsorbed on the electrode active sites [5].

The low electrocatalytic activity of deposit **2** relative to 1,4-BQ oxidation (Fig. 1, curve 2(**1**) is probably due to the presence of perchlorate ions doping the PbO_2. Nielsen *et al.* [27] have demonstrated that the chlorine element, doubtless in the form of perchlorate ions, is present in lead dioxide prepared from an electrolytic solution of perchloric acid. Ho and Hwang [28] have shown that acetate doped PbO_2 has a higher electrocatalytic activity for oxygen evolution than pure PbO_2. By analogy, the strong inhibition of the 1,4-benzoquinone oxidation reaction on perchlorate doped PbO_2 can be seen in terms of a competition with the formation of molecular oxygen. Keeping in mind that phenol oxidation to hydroquinone occurs at the same rate on perchlorate doped PbO_2 as on pure PbO_2, the organic compounds adsorb onto the electrode, in all probability, at specific sites which are identical for both materials. In the case of perchlorate doped PbO_2, certain sites are occupied by perchlorate ions and do not take part in the oxygen atom transfer reactions. Overall, perchlorate doping of PbO_2 corresponds to a decrease in the active surface available for the oxidation of intermediate products of phenol degradation and an increase in the electrocatalytic activity of the electrode for the oxygen evolution.

The effect of doping lead oxide with bismuth on its efficiency in phenol degradation has been studied as a function of the value of the concentrations ratio $R_c = [Bi^{3+}]/[Pb^{2+}]$ in the solution used for the preparation of the Bi_2O_5–PbO_2 (Table 1). Two electrolyses of a phenol solution have thus been carried out on Bi–PbO_2 for R_c values of 0.02 and 0.5 (deposits **3** and **4**, respectively); the results obtained have been compared with those found for anode **2** doped only with perchlorate (Fig. 2). Doping of the lead dioxide with bismuth has practically no significant effect on the kinetics of the first oxidation step of phenol to hydroquinone; the curves showing the increase of 1,4-benzoquinone concentration are practically the same. This effect is in relation with the mass transport limitation of the first step of phenol oxidation [5]. However, the charge needed for the consumption of 1,4-benzoquinone on Bi–PbO_2 (deposits **3** and **4**; curves 2(**3**) and 2(**4**), respectively) is less than that required on perchlorate doped PbO_2 (deposit N° **2**; curve 2(**2**)). Nonetheless, in spite of this positive effect of doping PbO_2 with bismuth on oxygen atom transfer reactions, the complete consumption of 1,4-benzoquinone on Bi_2O_5–PbO_2 needs a much higher charge ($110\,Ah\,dm^{-3}$) than that found for pure PbO_2 ($50\,Ah\,dm^{-3}$ for curve 2(**1**) in Fig. 1).

The work of Nielsen *et al.* [27] has shown that one of the consequences of bismuth doping is an increase in the amount of chlorine incorporated into the Bi–PbO_2. They have concluded that, in the presence of perchloric acid, bismuth is codeposited at its oxidation state Bi(v) in the form of $BiO_2(ClO_4)$. On the other hand, the higher the quantity of codeposited bismuth, the lower the oxygen evolution overpotential ηO_2 of Bi–PbO_2; the increase in the electrocatalytic activity of PbO_2 by doping with bismuth is thus directly correlated with ηO_2 [15, 19]. We can consider that differences in the apparent oxygen-evolution overpotential might be the result of differences in surface roughness. If one takes into account the oxygen overvoltage decrease of Bi–PbO_2 as a function

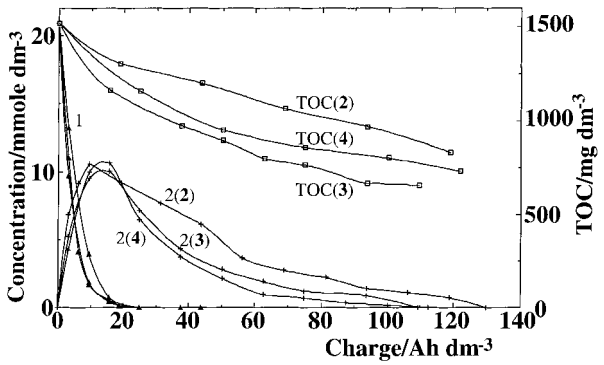

Fig. 2. Variation of the concentration of phenol, 1,4-benzoquinone and TOC during the electrochemical oxidation of phenol. Anodes **2**: PbO_2 ($HClO_4$); **3** and **4**: Bi–PbO_2 (see Table 1). Same conditions as in Fig. 1. Key: (1) phenol; (2(**2**), 2(**3**) and 2(**4**)) 1,4-benzoquinone; (TOC(**2**), TOC(**3**) and TOC(**4**)) total organic carbon.

of the value of the ratio R_c, doping PbO_2 with bismuth should logically favour oxygen evolution. Nonetheless, the improvement in the performance of PbO_2 for oxygen transfer reactions, when it is doped with bismuth, is doubtless due to an increase in the concentration of adsorbed hydroxyl radicals if the process is limited by the competition with the parasite reaction giving molecular oxygen rather than by mass transport of the reactant [5].

Overall, doping lead dioxide with bismuth could have a catalytic effect linked to the role of bismuth in the oxide mixture [18, 19]. Conversely, the material prepared in a perchloric acid medium does not perform as well as pure PbO_2 due to the inhibiting effect of the perchlorate ions in the oxygen transfer reactions.

Figure 3 shows that maleic acid is very resistant to oxidation as much on perchlorate doped PbO_2 as on Bi_2O_5–PbO_2. The curves for the variation in total organic carbon during the electrolysis of phenol (Fig. 2) show that the bismuth doped PbO_2 has an overall catalytic effect on the conversion of phenol to CO_2 and H_2O. Nevertheless, the efficiency of the elimination of total organic carbon on perchlorate doped PbO_2 and on Bi_2O_5–PbO_2 is still very low relative to that obtained with pure PbO_2 (Fig. 1; curve TOC(**1**)).

At the end of electrolysis, the deposits of Bi_2O_5–PbO_2 **3** and **4** become black, but they retain their mechanical properties and remain adherent to the substrate. Assaying lead and bismuth in solution reveal, at the beginning of the electrolyses, a rapid and monotonics selective dissolution of the lead dioxide followed by that of the bismuth oxide. The concentration of bismuth remains at zero up to 50 Ah dm^{-3} and then rises rapidly to 25 mmol dm^{-3} when a charge of 120 Ah dm^{-3} is passed (Fig. 4). The corrosion of the Bi–PbO_2 electrode is probably due to the oxygen evolution which increases as the concentration of organic compounds in solution decreases.

As in the case for the PbO_2 electrodes (deposits **1** and **2**) and the Bi_2O_5–PbO_2 electrodes (deposits **3** and **4**), the complete consumption of phenol on PbO_2/Bi_2O_5–PbO_2 (deposits **5** and **6**) occurs after passing about 20 Ah dm^{-3}; the rate of phenol consumption is thus independent of the amount of doping in the Bi_2O_5–PbO_2 layer underlying the PbO_2 deposit (Fig. 5). On the other hand, the higher the value of the ratio R_c, the maximum concentration and the charge necessary for the 1,4-benzoquinone elimination are higher. Fig. 6 clearly shows the inhibiting effect of the perchlorate ions on the performance of bismuth doped lead oxide. Indeed, on Fig. 6, curves 3(**5**), 3(**6**) and 3(**1**) show the difficulty in maleic acid oxidation on Bi_2O_5–PbO_2 compared to pure PbO_2. The slow conversion rate of phenol to CO_2 and H_2O and the consequent modest level of total organic carbon elimination at the end of the electrolysis (Fig. 5) stem from this inhibiting effect.

At the end of the electrolysis, deposits **5** and **6** become detached from the substrate in places. At the beginning of the electrolysis, deposit **6** is the center for a rapid and selective dissolution of bismuth (Fig. 7). The lead dioxide sites have, on the other hand, shown good stability at the beginning of the electrolysis followed by some light corrosion. Deposits **5** and **6** have a similar behaviour except that the lead dioxide sites of the deposit **5** are also corroded at the beginning of the electrolysis (Fig. 7).

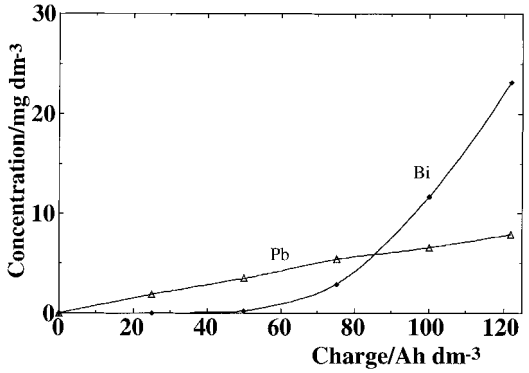

Fig. 4. Variation of the concentrations of lead and bismuth during the electrolyses of phenol on Bi–PbO_2 anodes (S = 20 cm^2, deposits **3** and **4**); see details in Table 1. Same conditions as in Fig. 1.

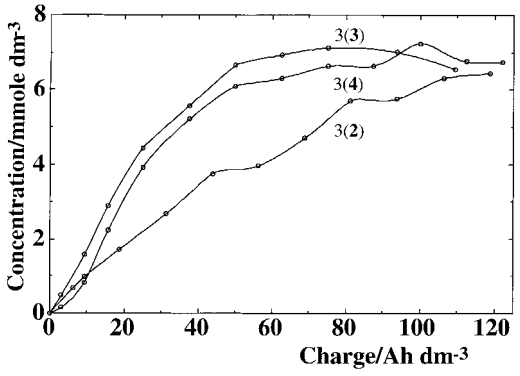

Fig. 3. Variation of the concentration of maleic acid during the electrochemical oxidation of phenol on anodes (S = 20 cm^2). Key: (**2**) PbO_2 ($HClO_4$); (**3**): Bi–PbO_2 (R_c = 0.02) and (**4**) Bi–PbO_2 (R_c = 0.5); see Table 1. Same conditions as in Fig. 1.

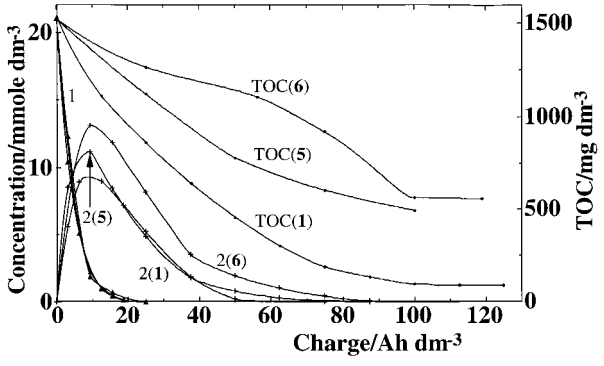

Fig. 5. Variation of the concentration of phenol, 1,4-benzoquinone and TOC during the electrochemical oxidation of phenol. Anodes (S = 20 cm^2): PbO_2 (deposit **1**), Bi–PbO_2 (deposits **5** and **6**); see details in Table 1. Same conditions as in Fig. 1. Key: (1) phenol; (2(**1**), 2(**5**) and 2(**6**)) 1,4-benzoquinone; (TOC(**1**), TOC(**5**) and TOC(**6**)) total organic carbon.

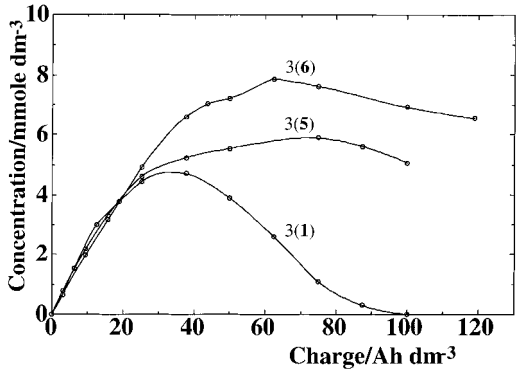

Fig. 6. Variation of the concentration of maleic acid during the electrochemical oxidation of phenol. Anodes ($S = 20\,cm^2$): PbO_2 (deposit **1**); Bi–PbO_2 (deposits **5** and **6**); see details in Table 1. Same conditions as in Fig. 1.

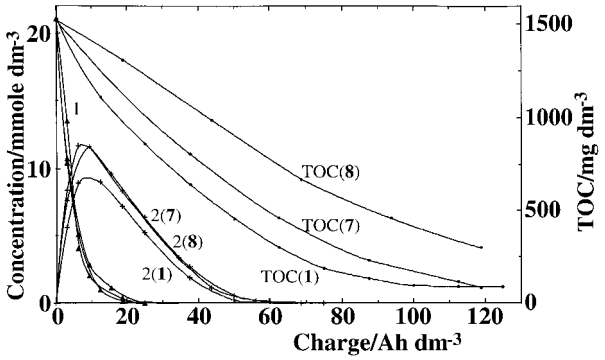

Fig. 8. Variation of the concentration of phenol, 1,4-benzoquinone and TOC during the electrochemical oxidation of phenol. Anodes ($S = 20\,cm^2$): PbO_2 (deposit **1**); Bi–PbO_2 (deposits **7** and **8**); see details in Table 1. Same conditions as in Fig. 1. Key: (1) phenol; (2(**1**), 2(**7**) and 2(**8**)) 1,4-benzoquinone; (TOC(**1**), TOC(**7**) and TOC(**8**)) total organic carbon.

These results mean that the bismuth sites in the Bi_2O_5–PbO_2 layer underlying the lead dioxide deposit are very electroactive concerning oxygen evolution. The resulting gaseous oxygen evolution inside the electrode is probably the cause of the deterioration of the deposit which becomes detached from the substrate in places. The strong selective dissolution of the bismuth for $R_c = 0.1$ (Fig. 7; curve Bi(**5**)) compared with that found for $R_c = 0.5$ (Fig. 7; curve Bi(**6**)) can be interpreted as a greater oxygen evolution on the bismuth sites because of their lower surface density.

As has already been stated, the Bi_2O_5–PbO_2 electrodes prepared from a perchloric acid electrolyte solution, do not allow the effect of doping with bismuth alone on the electrocatalytic properties of lead dioxide to be studied. The Bi_2O_5–PbO_2 electrodes (deposits **7** and **8**) have thus been prepared using electrolytic solutions which do not contain perchloric acid; the concentrations of bismuth nitrate are low ($R_c = 2 \times 10^{-4}$ and 2×10^{-3}) for deposits of Bi_2O_5–PbO_2 **7** and **8**, respectively, because of its low solubility in water.

Figure 8 shows that the charges corresponding to the total consumption of phenol and of the 1,4-benzoquinone are hardly affected by the bismuth doped PbO_2. However, the rate of phenol conversion into carbon dioxide and water is considerably slowed down by the doping effect. Figure 9 confirms the inhibiting effect of bismuth doped lead oxide: the higher the degree of doping the more difficult it is to oxidize the maleic acid.

At the end of the electrolysis, the two deposits are intact and adhere to the substrate. The study of the stability of deposit **8** reveals a corrosion behaviour identical to that of deposit **6**. For deposit **7**, no dissolution was observed within the detection limits of the ICP analyser.

4. Conclusion

This study has shown the negative effect of perchlorate doped PbO_2 on the transfer of oxygen atoms. The adsorption of perchlorate ions on the lead dioxide sites results in an increase in the electrolytic activity of the electrode for oxygen evolution; the oxidation of organic compounds on perchlorate doped PbO_2 is limited by a strong competition with the parasite reaction of molecular oxygen formation.

Overall, the doping of lead oxide with bismuth, performed using an electrolytic solution with or without perchloric acid, has an inhibiting effect on

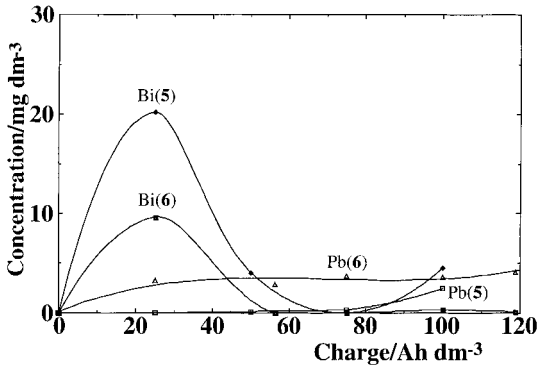

Fig. 7. Variation of the concentrations of lead and bismuth during the electrolyses of phenol on a Bi–PbO_2 anodes ($S = 20\,cm^2$): deposits **5** and **6** (see details in Table 1). Same conditions as in Fig. 1.

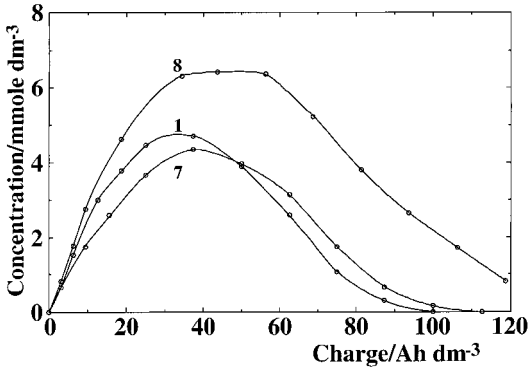

Fig. 9. Variation of the concentration of maleic acid during the electrochemical oxidation of phenol. Anodes ($S = 20\,cm^2$): PbO_2 (deposit **1**); Bi–PbO_2 (deposits **7** and **8**). Same conditions as in Fig. 1.

the oxygen atom transfer; the electrodes of pure lead dioxide prepared from lead nitrate in aqueous solution without any perchlorate ions give always the best performances.

Acknowledgements

This work was partially supported by the Région Midi Pyrénées (CCRRDT, File RECH/9308175, 16 Aug. 1994), and by the Comité Mixte Franco–Tunisien pour la Coopération Universitaire (Projet 96/F 11 13).

References

[1] J. E. Vitt and D. C. Johnson, *J. Electrochem. Soc.* **139** (1992) 774.
[2] Ch. Comninellis and C. Pulgarin, *J. Appl. Electrochem.* **23** (1993) 108.
[3] N. Belhadj Tahar, Thesis, Université Paul Sabatier, Toulouse (1996).
[4] N. Belhadj Tahar and A. Savall, *in* 'Fundamentals and Potential Applications of Electrochemical Synthesis', edited by R. D. Weaver, F. Fisher, F. R. Kalhammer and D. Mazur, (The Electrochemical Society, Pennington, NJ, 1997), pp. 198–206.
[5] N. Belhadj Tahar and A. Savall, submitted to *J. Electrochem. Soc.* **145** (1998) 3427.
[6] H. Sharifian and D. W. Kirk, *J. Electrochem. Soc.* **133** (1986) 921.
[7] M. Gattrell and D. W. Kirk, *Can. J. Chem. Eng.* **68** (1990) 997.
[8] Ch. Comninellis and C. Pulgarin, *J. Appl. Electrochem.* **121** (1991) 703.
[9] M. Gattrell and D. W. Kirk, *J. Electrochem. Soc.* **140** (1993) 1534.
[10] E. Brillas, R. M. Bastida and E. Liosa, *ibid.* **142** (1995) 1733.
[11] A. Savall and N. Belhadj Tahar, *in* 'Environmental Technologies and Trends', Proceed. Earthcare, edited by R. K. Jain, Y. Aurelle, C. Cabassud, M. Roustan and S. P. Shelton, (Springer-Verlag, Berlin, 1996), pp. 262–269.
[12] N. Belhadj Tahar and A. Savall, *J. New Mater. Electrochem. Syst.* (in press).
[13] B. Fleszar and J. Ploszynska, *Electrochim. Acta.* **30** (1985) 31.
[14] H. Chang and D. C. Johnson, *J. Electrochem. Soc.* **136** (1989) 17.
[15] I. H. Yeo, S. Kim, R. Jacobson and D. C. Johnson, *ibid.* **136** (1989) 1395.
[16] Ch. Comninellis, *Electrochim. Acta* **39** (1994) 1857.
[17] J. Feng, L. L. Hook and D. C. Johnson, *J. Electrochem. Soc.* **142** (1995) 3626.
[18] I. H. Yeo and D. C. Johnson, *ibid.* **134** (1987) 1973.
[19] W. R. Lacourse, Y. L. Hsiao and D. C. Johnson, *ibid.* **136** (1989) 3714.
[20] J. C. Grigger, H. C. Miller and F. D. Loomis, *ibid.* **105** (1958) 100.
[21] K. C. Narasimham and H. V. K. Udupa, *ibid.* **123** (1976) 1294.
[22] N. Munichandraiah, and S. Sathyanarayama, *J. Appl. Electrochem.* **17** (1987) 22.
[23] N. Munichandraiah, *ibid.* **22** (1992) 825.
[24] J. Rolewicz, Ch. Comninellis, E. Plattner and J. Hinden, *Electrochim. Acta.* **33** (1988) 573.
[25] L. Papouchado, R. W. Sandford, G. Petrie and R. N. Adams, *J. Electroanal. Chem.* **65** (1975) 275.
[26] M. Fleischmann, I. R. Hill, G. Mengoli and M. M. Musiani, *Electrochim. Acta.* **28** (1983) 1545.
[27] B. S. Nielsen, J. L. Davis and P. A. Thiel, *J. Electrochem. Soc.* **137** (1990) 1017.
[28] C. N. Ho and B. J. Hwang, *Electrochim. Acta.* **38** (1993) 2749.